Electronic Supplementary Information

Schottky DC Generators from Polypyrrole Nanocomposite of N-type Semiconductor Metal Oxides and Multiple Device Connection Effect

Xiang Ding [a], Hao Shao [a], Hongxia Wang [a], Haibo Chang [b], Ruixi Bai [a], Jian Fang [c], Weidong Yang [d], Tong Lin [e,*]

[a] Institute for Frontier Materials, Deakin University, Geelong, VIC 3216, Australia
[b] Institute of Functional Polymer Composites, College of Chemistry and Chemical Engineering, Henan University, Kaifeng 475004, China.
[c] College of Textile and Clothing Engineering, Soochow University, Suzhou, 215123, China
[d] Future Manufacturing Flagship, CSIRO, Clayton South, VIC 3169, Australia
[e] State Key Laboratory of Separation Membranes and Membrane Processes/Institute for Nanofiber Intelligent Manufacture and Applications, School of Textile Science and Engineering, Tiangong University, Tianjin 300387, China

*Corresponding author: Tong Lin; E-mail: tong.lin@tiangong.edu.cn

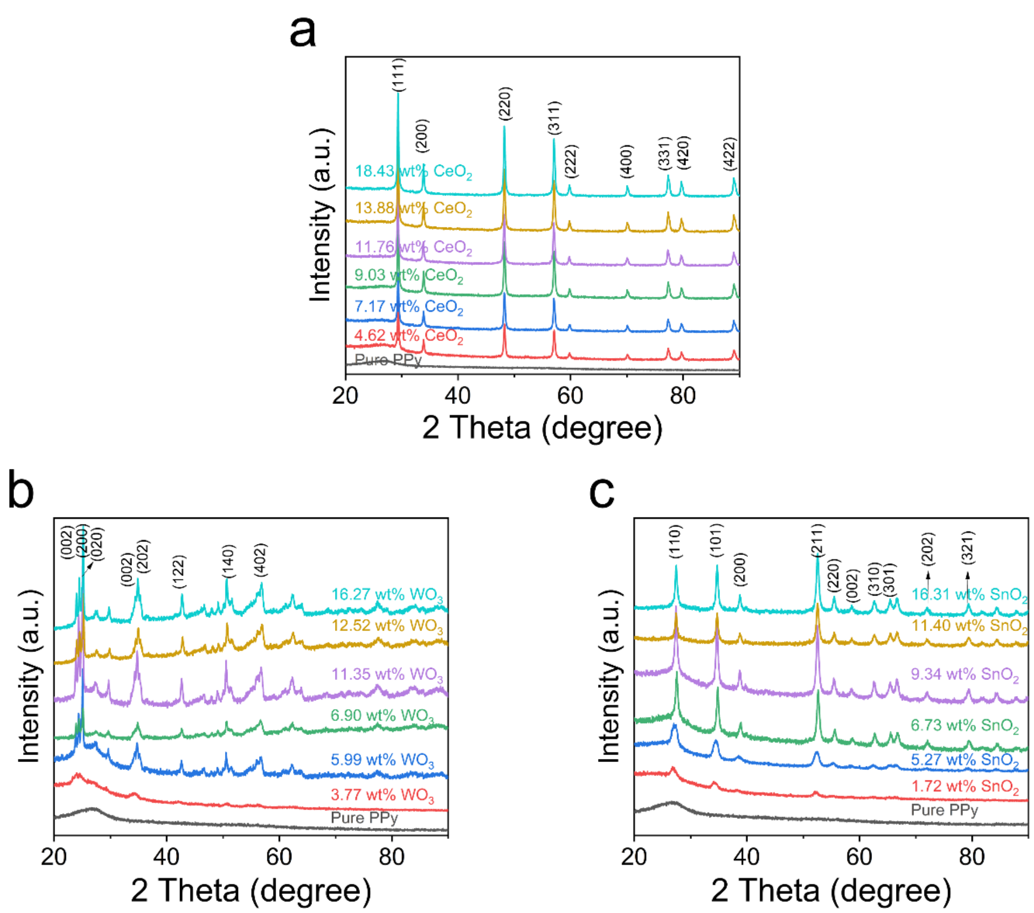

Fig. S1 XRD patterns of (a) PPy-CeO_2, (b) PPy-WO_3, and (c) PPy-SnO_2 nanocomposites with different metal oxide contents.

For PPy-CeO_2, the peaks at $2\theta = 28.27°$, 33.09°, 47.34°, 56.36°, 59.36°, 69.43°, 76.74°, and 79.74° were assigned to the (111), (200), (220), (311), (222), (400), (331) and (422) crystal planes of CeO_2, respectively. All peaks are in good agreement with the standard CeO_2[1].

For PPy-WO_3, the peaks of nanocomposite at $2\theta = 23.1°$, 23.6°, 24.4°, 26.6°, 28.9°, 33.3°, 34.2°, and 36.2° corresponded to the (002), (020), (200), (120), (112), (022), (202), and (212) planes of monoclinic WO_3[2].

For PPy-SnO_2, the peaks at $2\theta = 26.49°$, 33.77°, 38°, 51.72°, 54.78°, 57.95°, 61.86°, 64.77°, and 66°, which are assigned to scattering from (110), (101), (200), (211), (220), (002), (310), (112) and (301) reflection planes of tetragonal SnO_2[3].

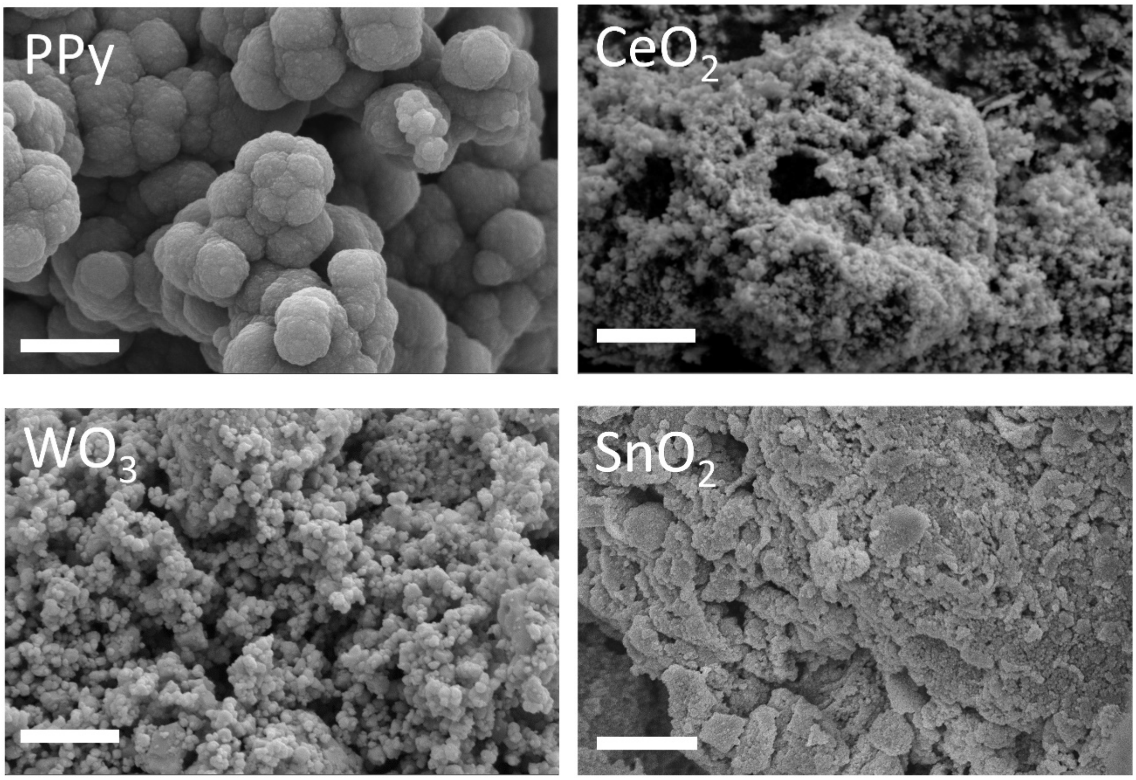

Fig. S2 SEM images of pure PPy and raw metal oxide materials (CeO_2, WO_3, and SnO_2) (scale bar: 1 μm).

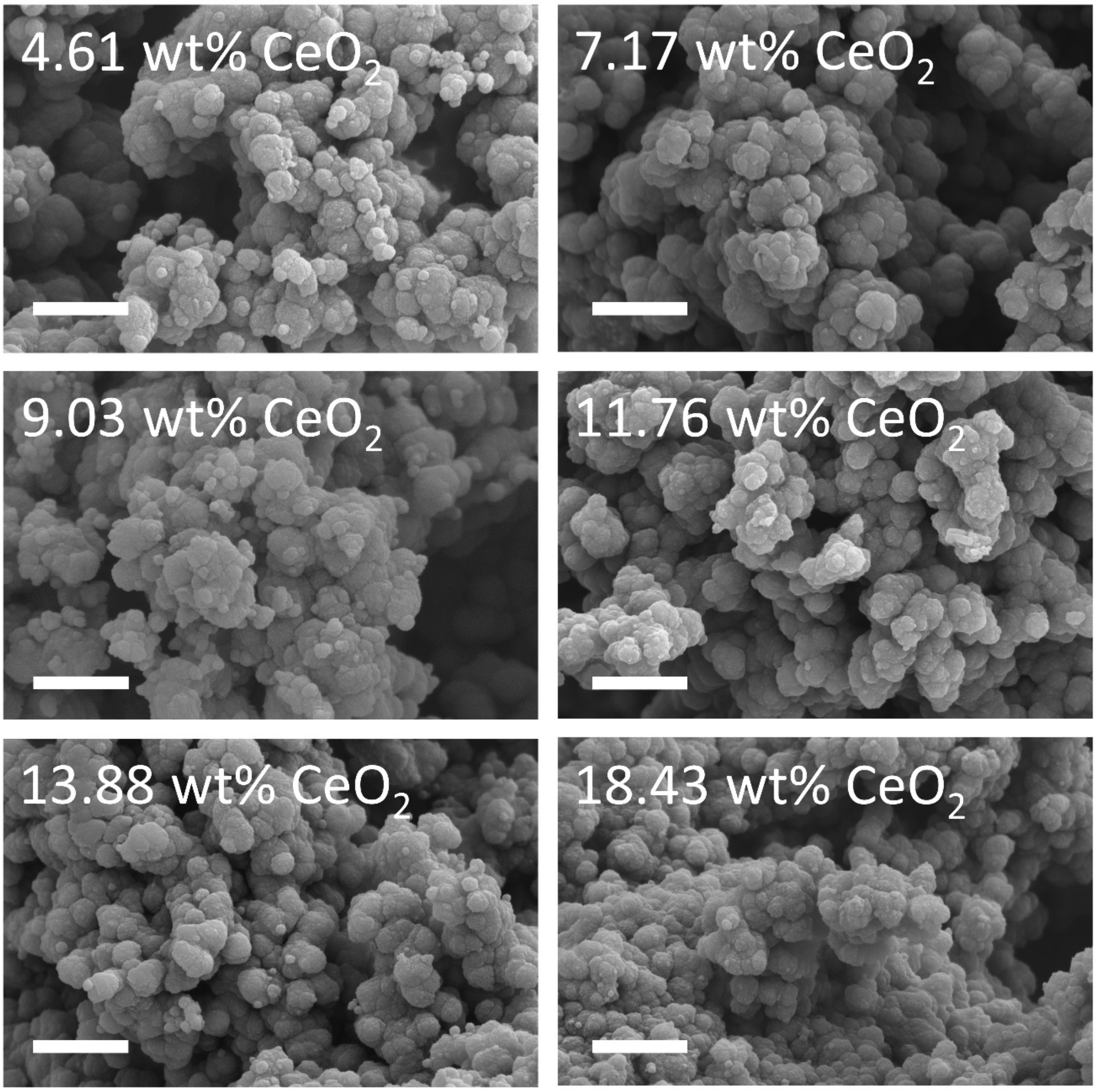

Fig. S3 SEM images of PPy-CeO_2 nanocomposites containing different CeO_2 contents (scale bar: 1 μm).

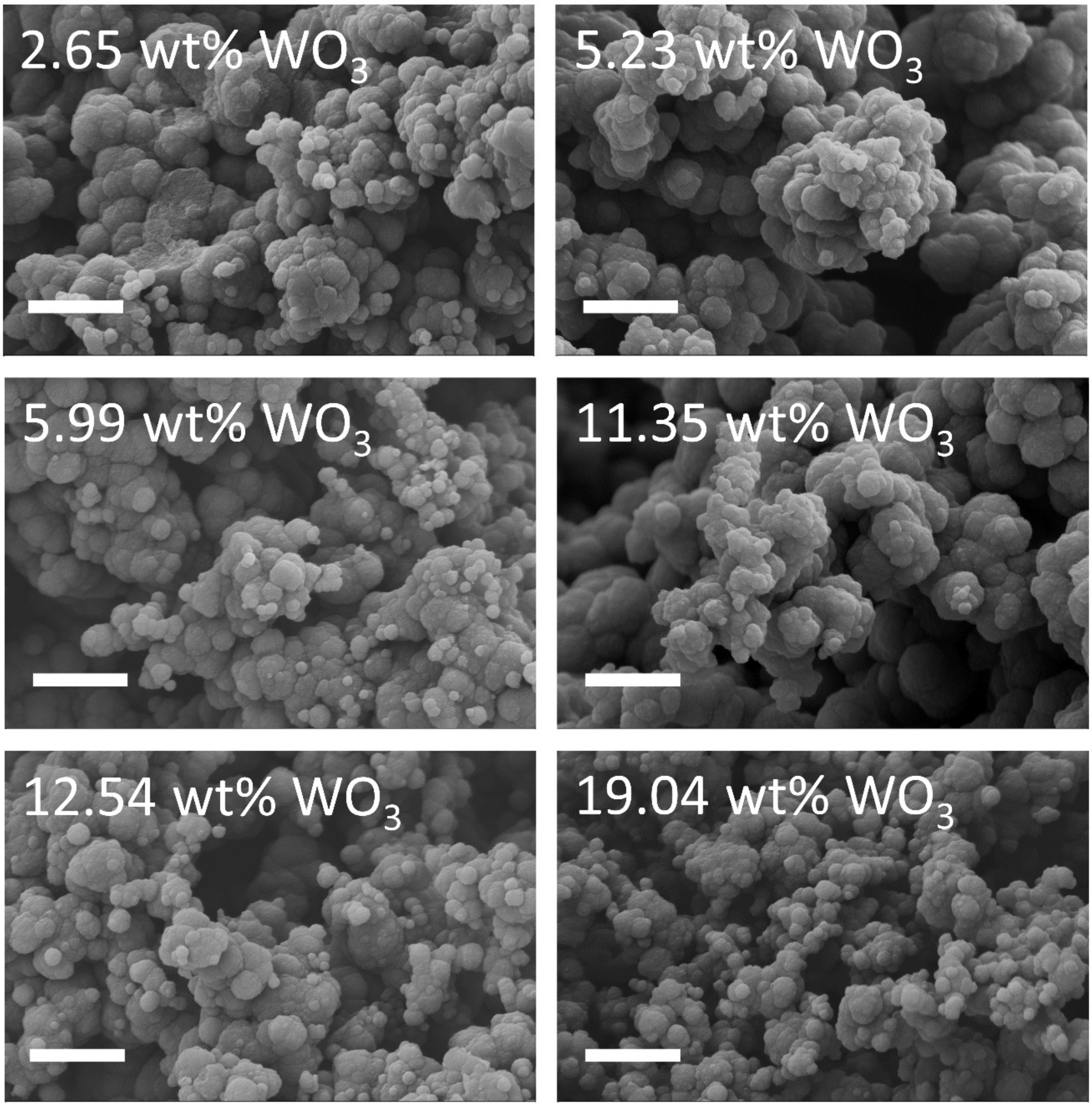

Fig. S4 SEM images of PPy-WO_3 nanocomposites containing different WO_3 contents (scale bar: 1 μm).

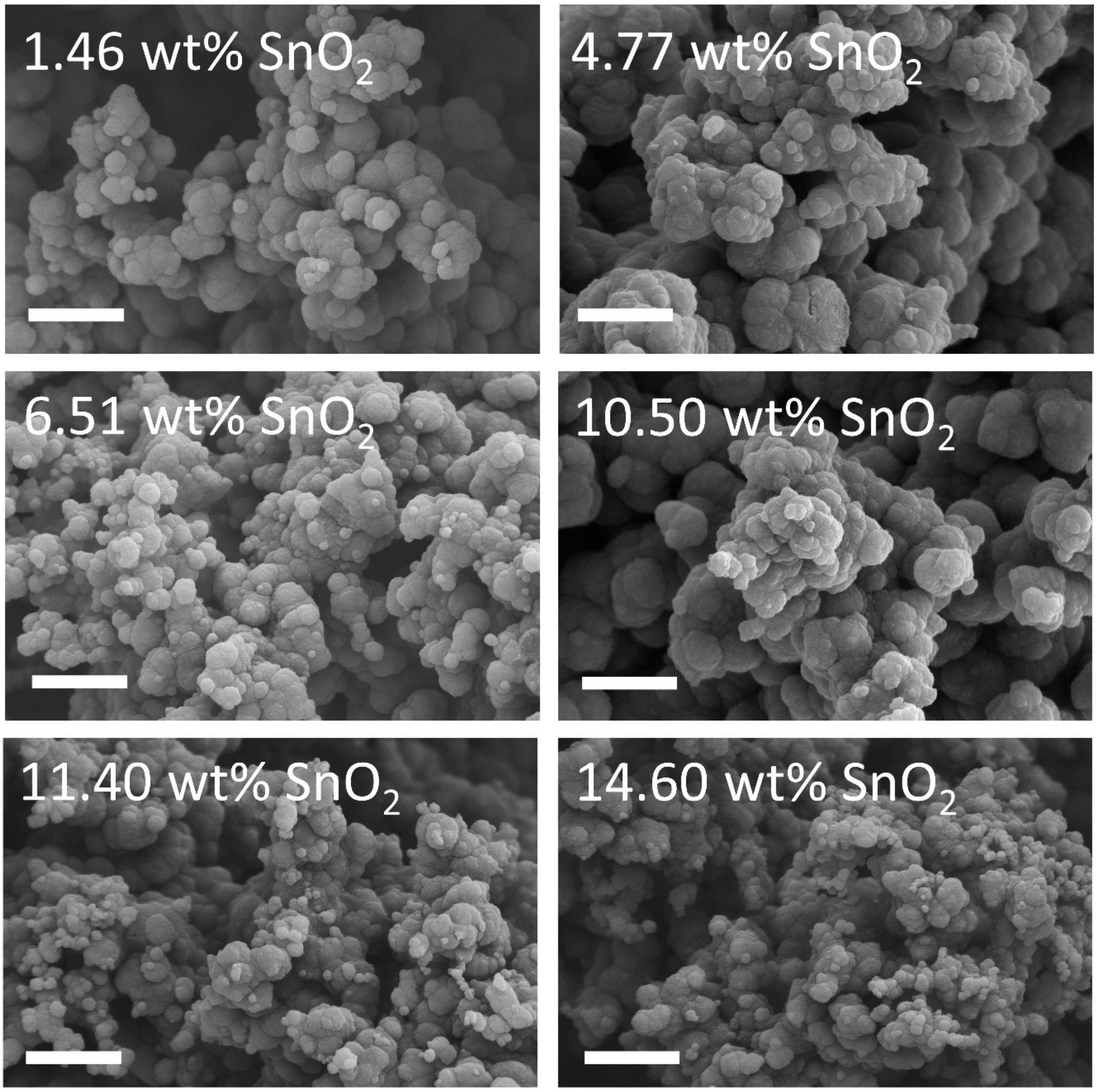

Fig. S5 SEM images of PPy-SnO_2 nanocomposites containing different SnO_2 contents (scale bar: 1 μm).

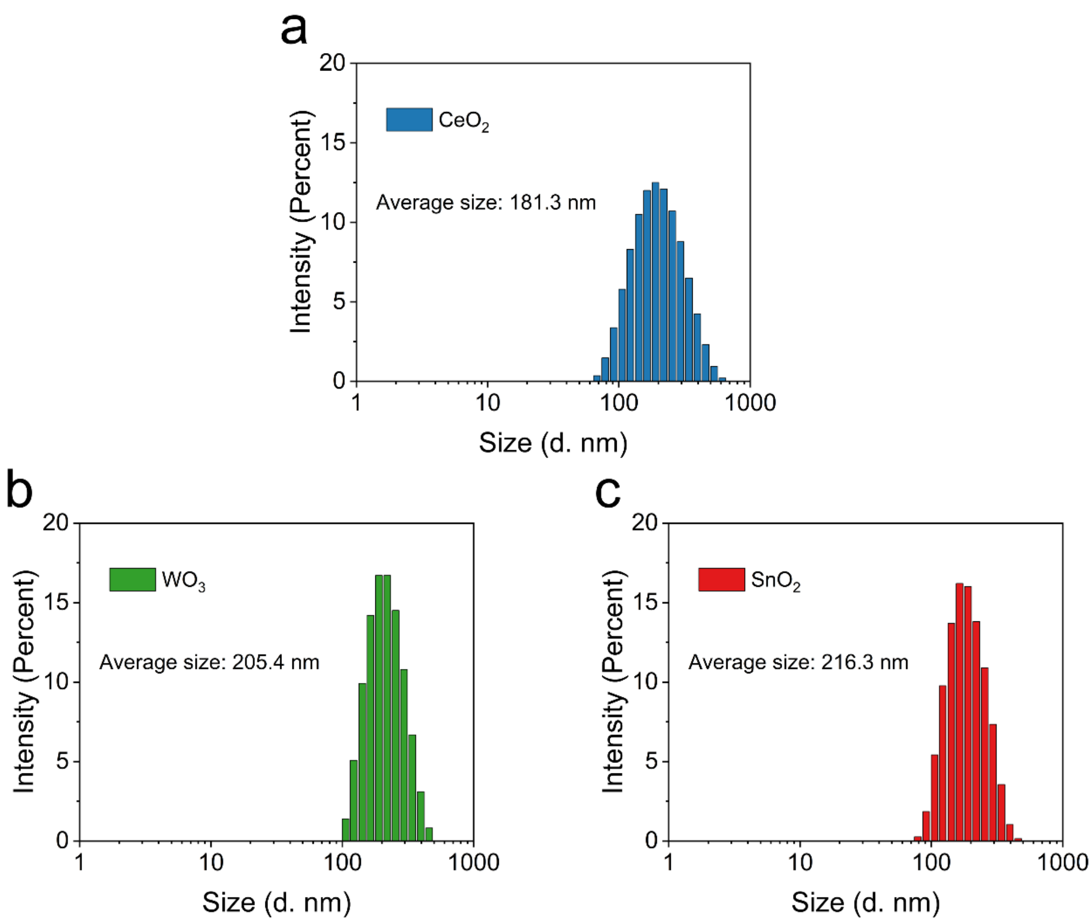

Fig. S6 Malvern Zetasizer Nano size measurement of (a) CeO_2, (b) WO_3, and (c) SnO_2 nanoparticles.

Table S1 BET surface area of raw metal oxide materials.

Materials	**CeO_2**	**WO_3**	**SnO_2**
BET surface area (m^2 g^{-1})	38.106	8.051	21.607

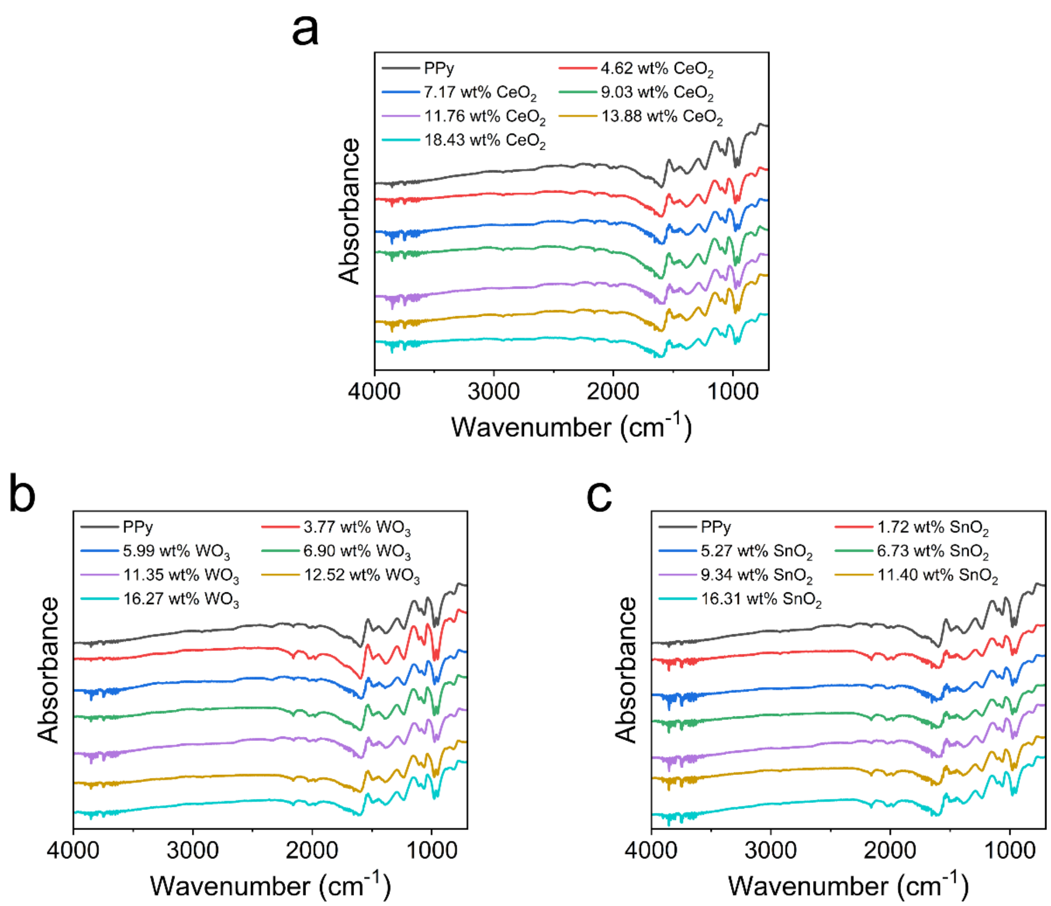

Fig. S7 FTIR spectra of (a) PPy-CeO_2, (b) PPy-WO_3, and (c) PPy-SnO_2 nanocomposites with different metal oxide contents.

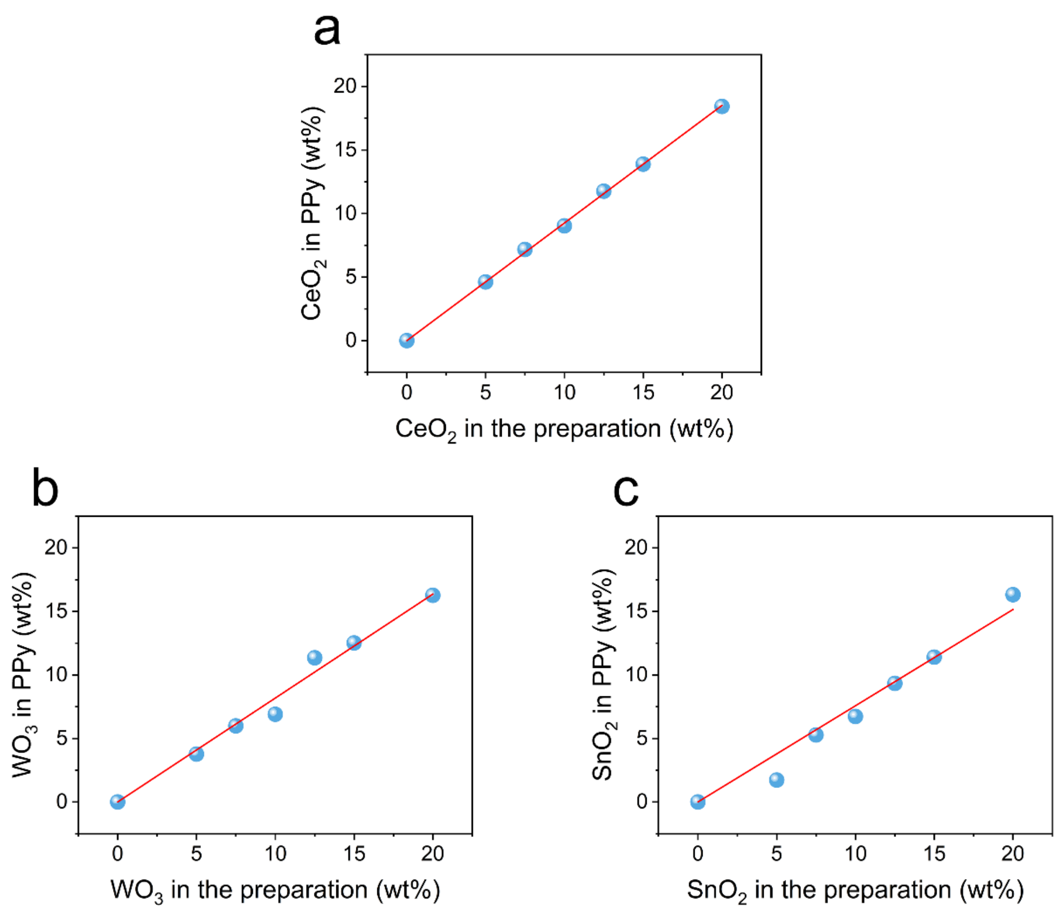

Fig. S8 Effect of (a) CeO_2, (b) WO_3, and (c) SnO_2 content in the PPy synthesis (based on pyrrole) on its actual content in the nanocomposites.

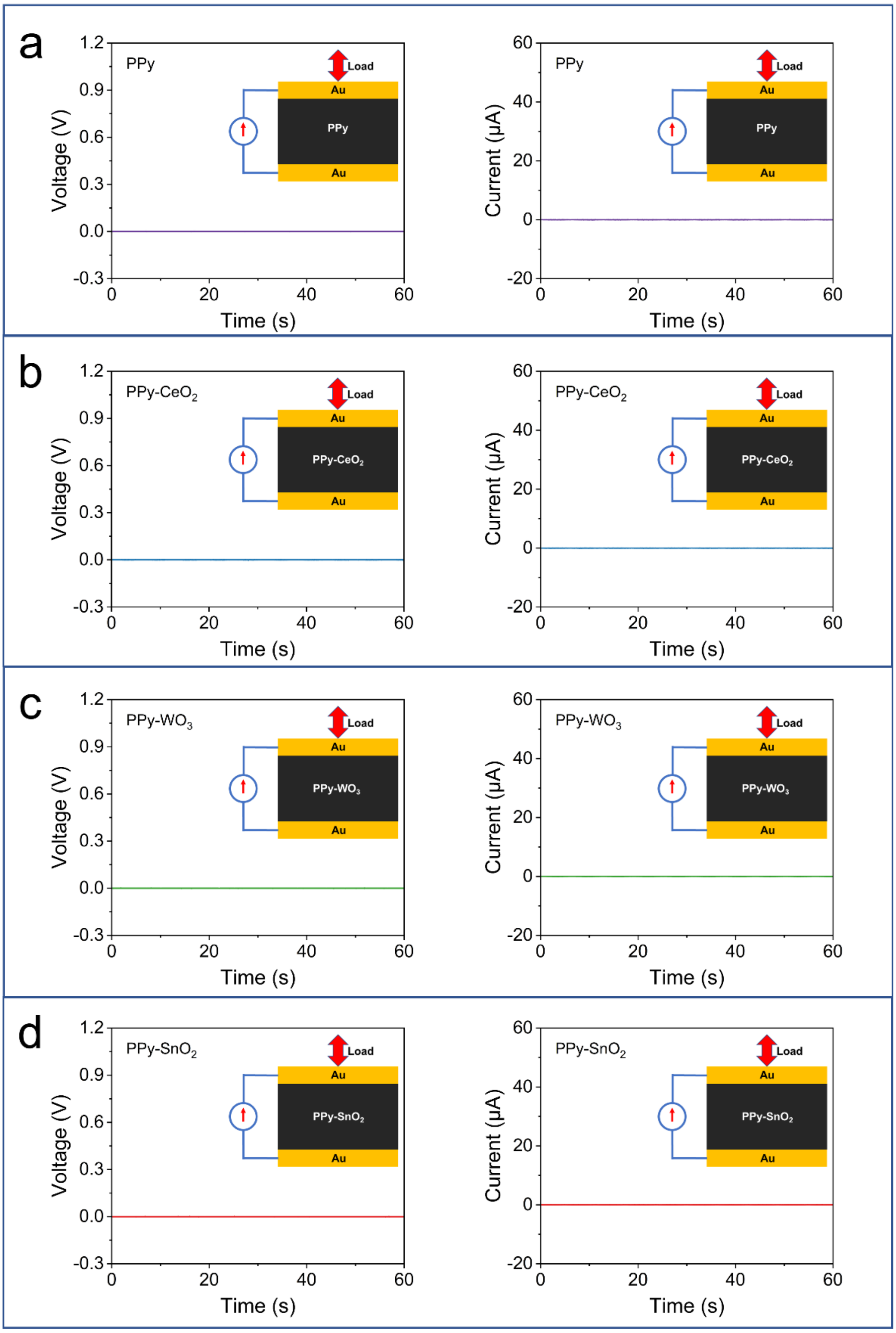

Fig. S9 Electrical response of (a) Au/PPy/Au, (b) Au/PPy-CeO_2/Au, (c) Au/PPy-WO_3/Au, and Au/PPy-SnO_2/Au devices under repeated compressive deformation (metal oxide content: 7.17 wt%, 6.90 wt%, and 6.73 wt% for PPy-CeO_2, PPy-WO_3, and PPy-SnO_2, strain rate: 6.0%, compressing & releasing speed: 0.035mm s^{-1}).

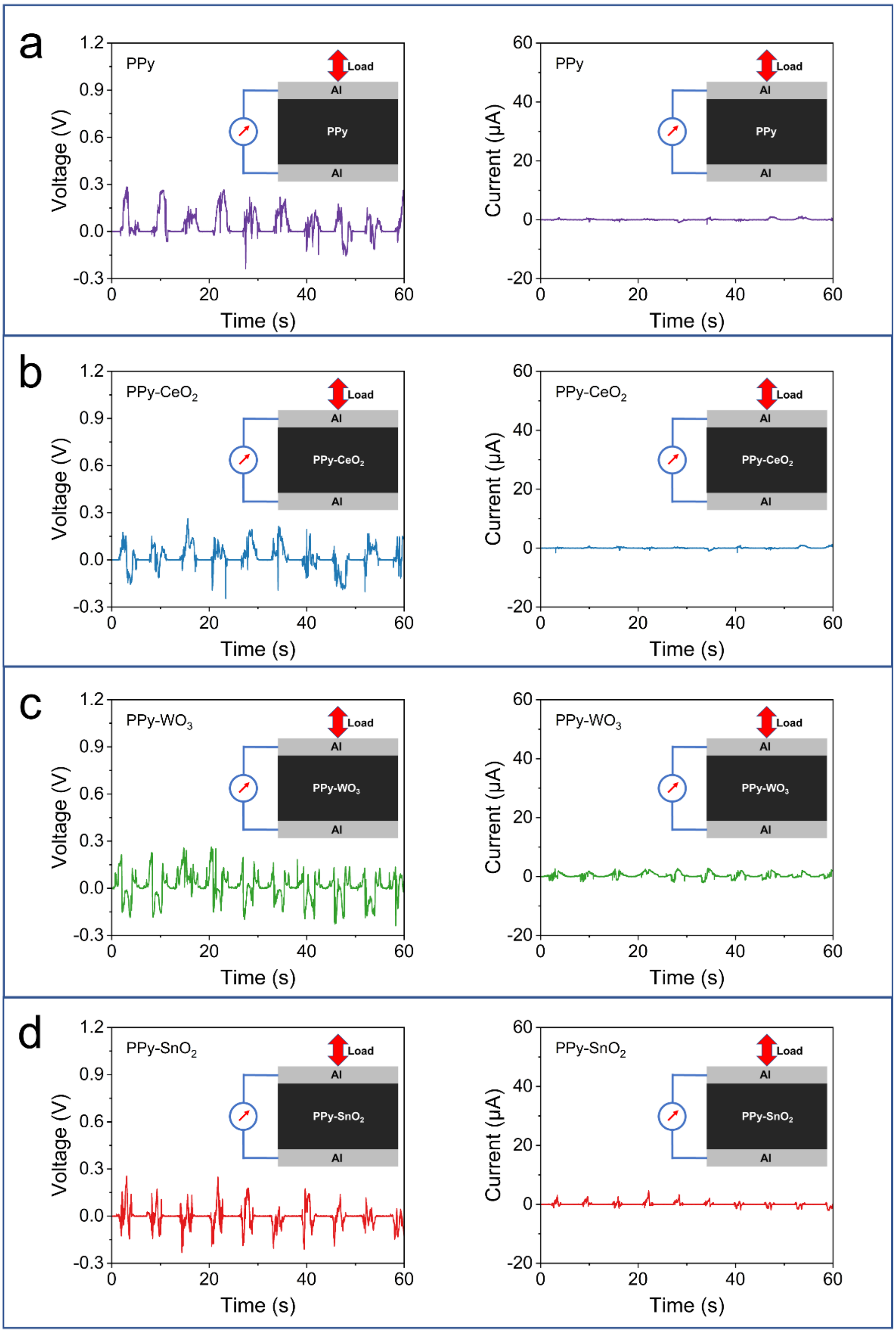

Fig. S10 Electrical response of (a) Al/PPy/Al, (b) Al/PPy-CeO_2/Al, (c) Al/PPy-WO_3/Al, and Al/PPy-SnO_2/Al devices under repeated compressive deformation (metal oxide content: 7.17 wt%, 6.90 wt%, and 6.73 wt% for PPy-CeO_2, PPy-WO_3, and PPy-SnO_2, strain rate: 6.0%, compressing & releasing speed: 0.035mm s^{-1}).

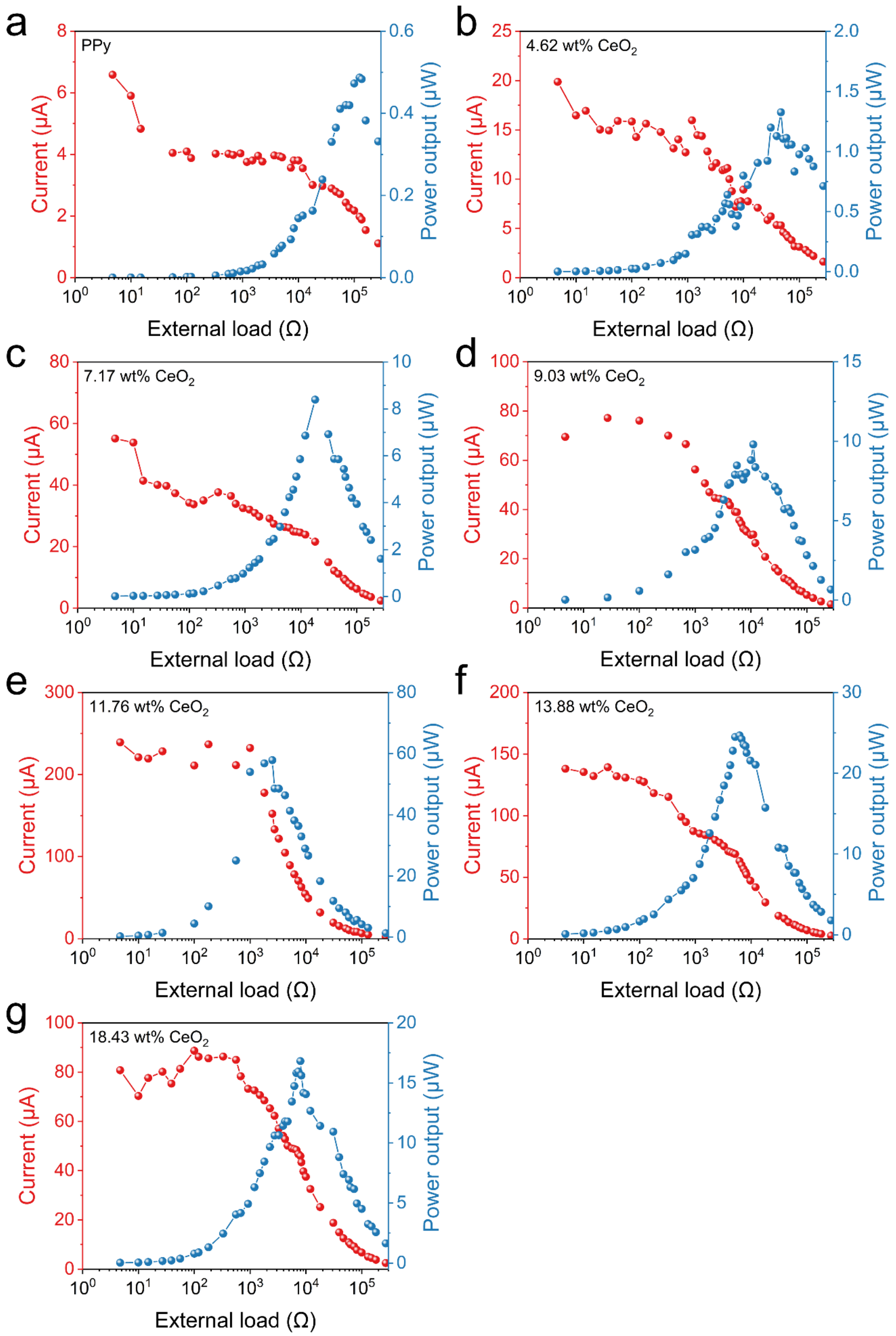

Fig. S11 Dependency of the current and power outputs on external resistances for PPy-CeO_2 devices with (a) 0 wt%, (b) 4.62 wt%, (c) 7.17 wt%, (d) 9.03 wt%, (e) 11.76 wt%, (f) 13.88 wt%, (g) 18.43 wt% CeO_2 in the nanocomposite.

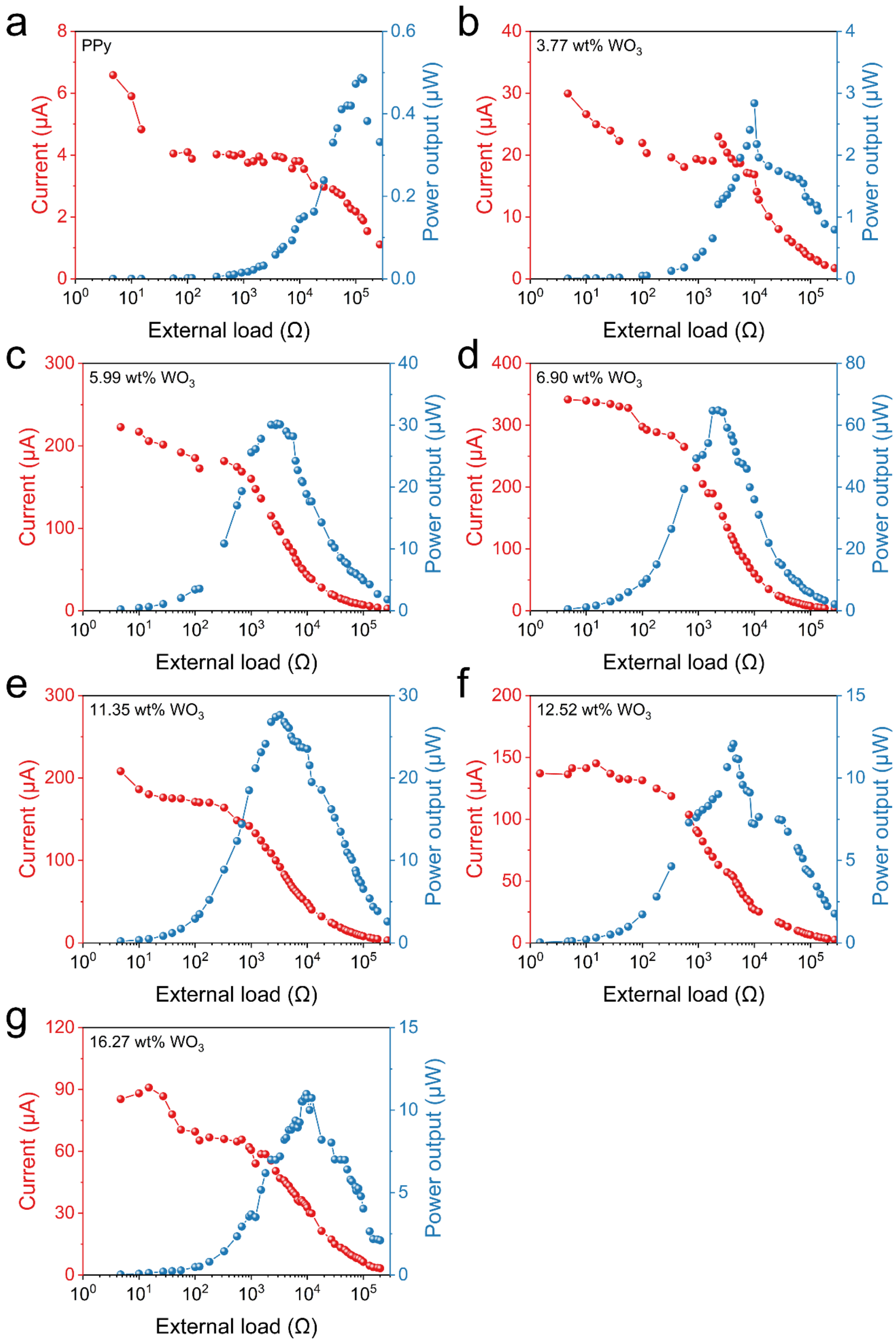

Fig. S12 Dependency of the current and power outputs on external resistances for PPy-WO_3 devices with (a) 0 wt%, (b) 3.77 wt%, (c) 5.99 wt%, (d) 6.90 wt%, (e) 11.35 wt%, (f) 12.52 wt%, (g) 16.27 wt% different WO_3 in the nanocomposite.

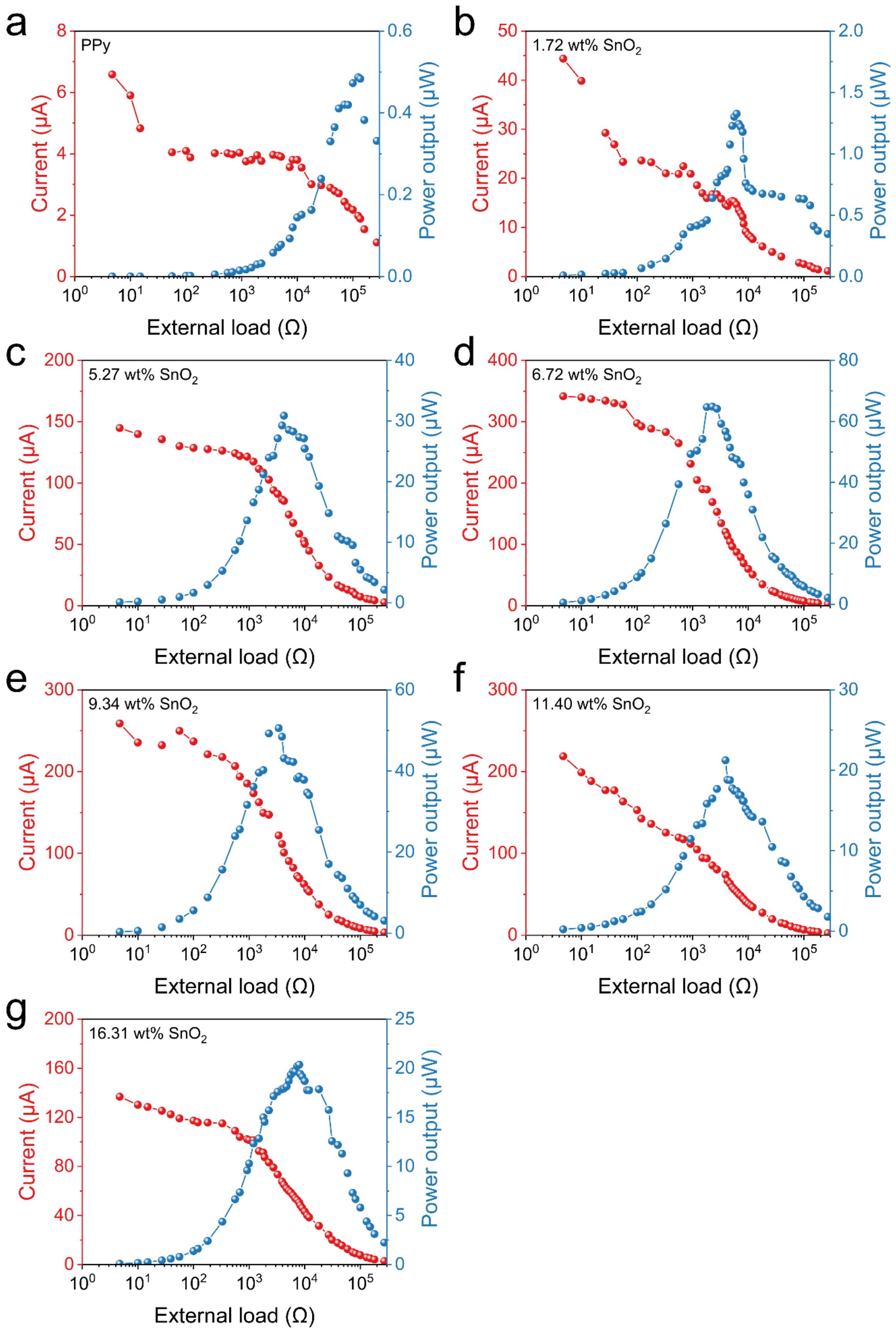

Fig. S13 Dependency of the current and power outputs on external resistances for PPy-SnO_2 devices with (a) 0 wt%, (b) 1.72 wt%, (c) 5.27 wt%, (d) 6.72 wt%, (e) 9.34 wt%, (f) 11.40 wt%, (g) 16.31 wt% SnO_2 in the nanocomposite.

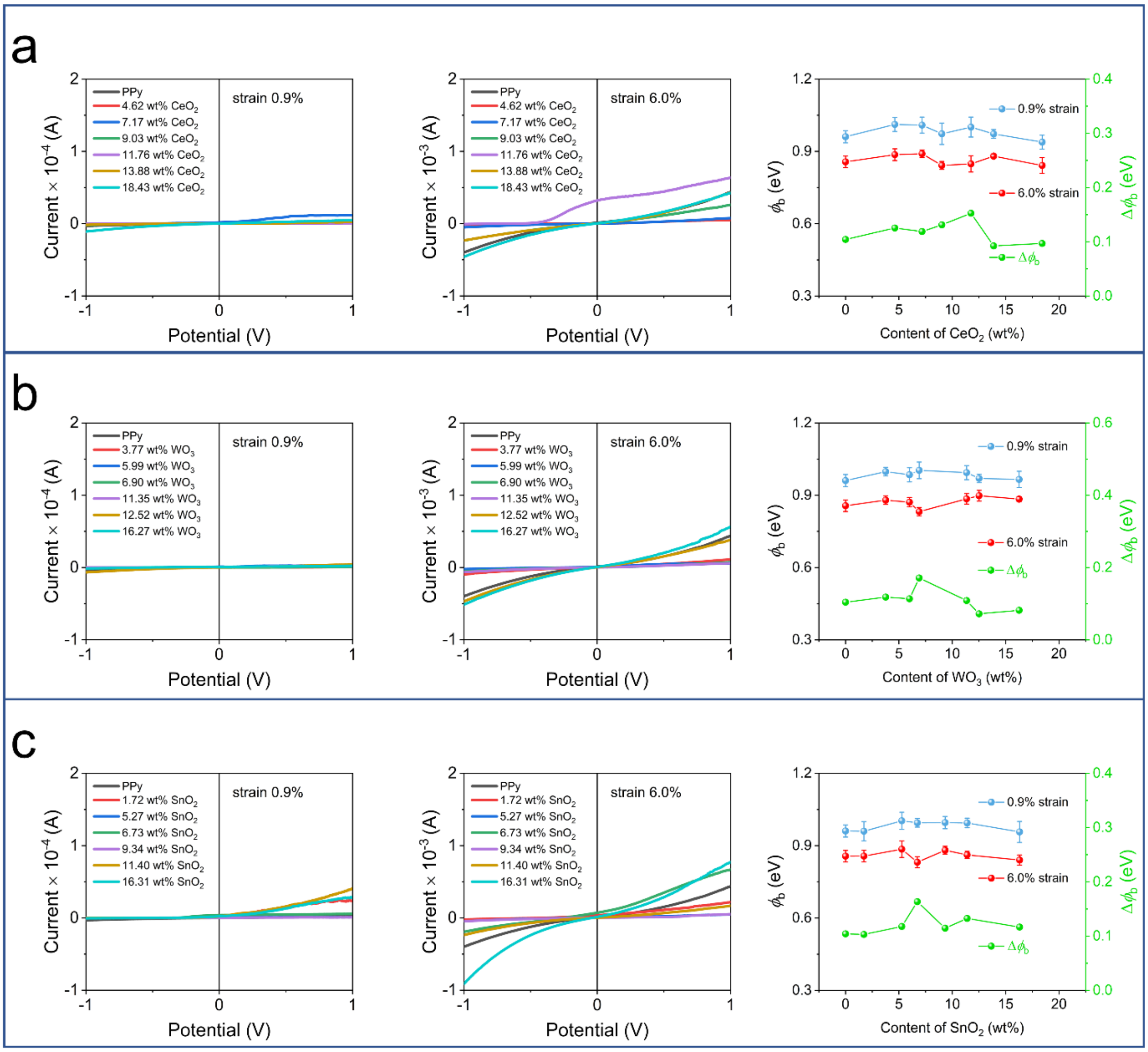

Fig. S14 I–V curves and calculated Schottky barrier height (ϕ_b) of (a) PPy-CeO_2, (b) PPy-WO_3, and (c) PPy-SnO_2 devices with different metal oxide contents (the Au/PPy-based nanocomposites/Al devices at the strain levels of 0.9% and 6.0%).

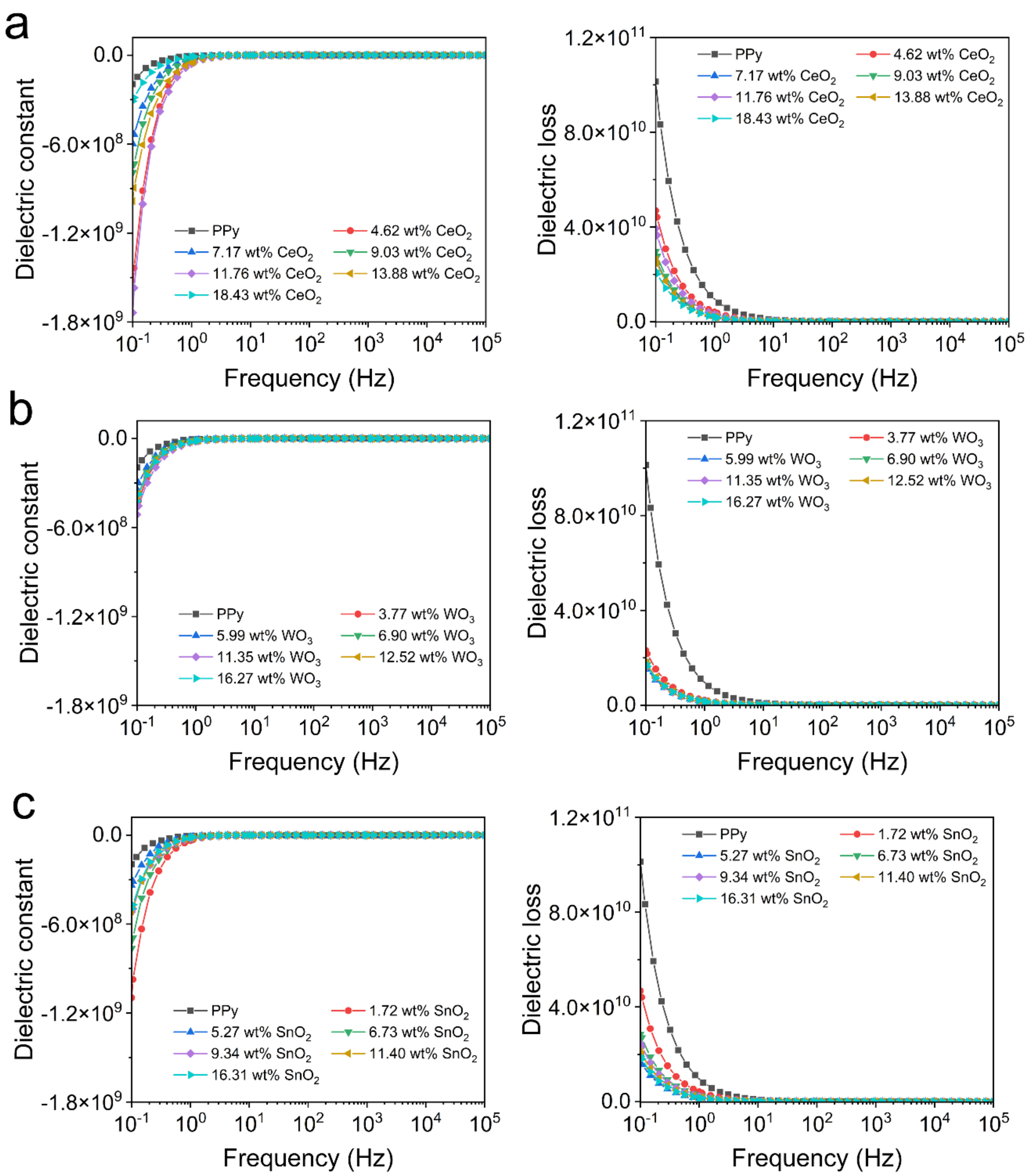

Fig. S15 The dielectric constant and dielectric loss of (a) PPy-CeO_2, (b) PPy-WO_3, and (c) PPy-SnO_2 nanocomposites with different metal oxide contents.

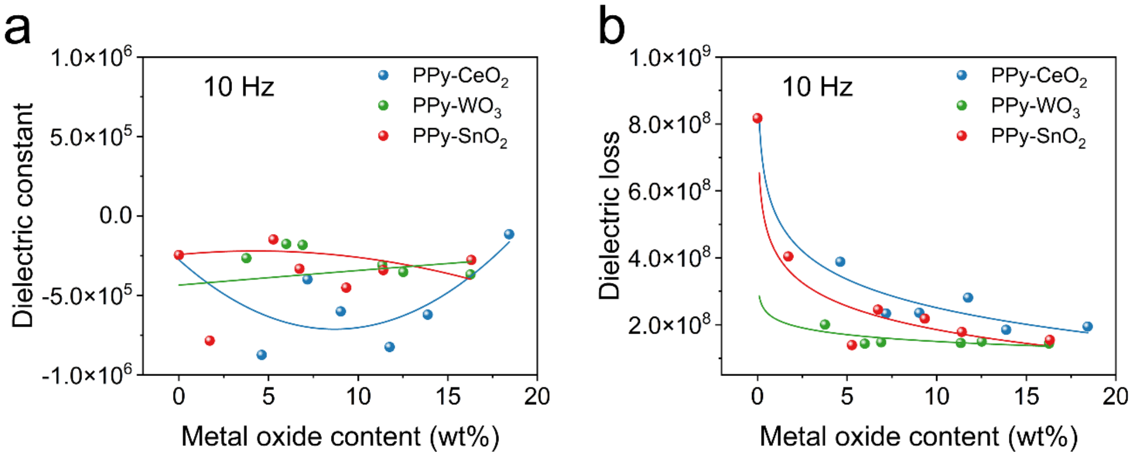

Fig. S16 Effect of CeO_2, WO_3, and SnO_2 content on (a) dielectric constant and (b) dielectric loss of the nanocomposites (at 10 Hz).

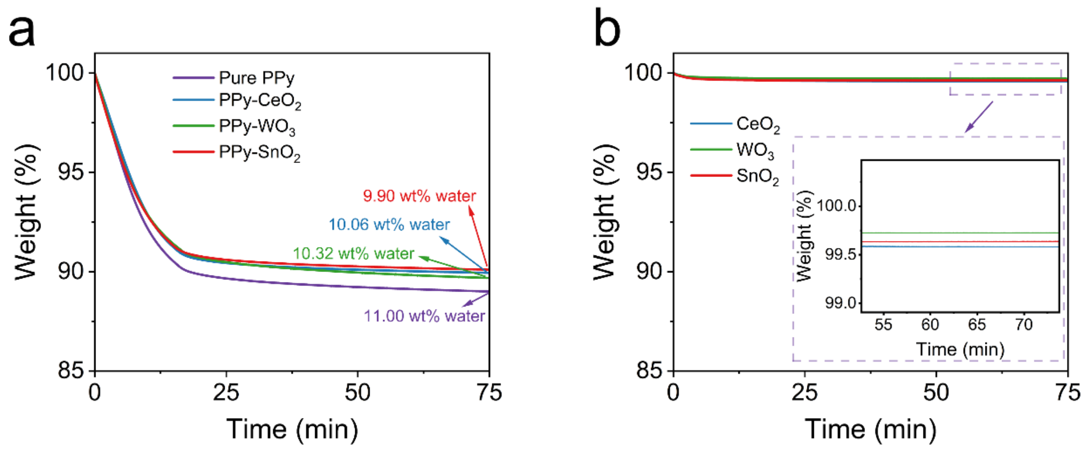

Fig. S17 (a) Weight loss of PPy and PPy nanocomposites (metal oxide content 7.17 wt%, 6.90 wt%, and 6.73 wt% for PPy-CeO_2, PPy-WO_3, and PPy-SnO_2) at 105 °C, (b) weight loss of three metal oxide powder at 105 °C.

The water content in PPy, PPy nanocomposites, and metal oxides was measured using a thermogravimetric analyzer (TGA, TA Q50). During testing, the weight loss was recorded by heating the sample to 105 °C (rate 5 °C min^{-1}) and heating the sample at 105 °C for 60 minutes. Under the same conditions, the water contents of PPy, PPy-CeO_2, PPy-WO_3, and PPy-SnO_2 were measured as 11.00 wt%, 10.06 wt%, 10.32 wt%, and 9.90 wt%, respectively. In comparison, the water content of the metal oxide powder was much lower, 0.42 wt%, 0.27 wt%, and 0.36 wt% for CeO_2, WO_3, and SnO_2, respectively. Because of the low water content in the metal oxide domain, the water content in the PPy domains was estimated by the equation:

$$WC_{PPy\ composites} = w_{PPy} * WC_{PPy} + w_{metal\ oxide} * WC_{metal\ oxide}$$

Here, *WC* is water content, *w* is the weight percent of each component in the composites. For PPy-CeO_2, the water content in the PPy domains should be (10.06%-7.17%*0.42%)/ 92.83% = 10.80 wt%. For PPy-WO_3 and PPy-SnO_2, the water content was 11.06 wt% and 10.59 wt%, respectively. These values were either similar to or lower than the water content in pure PPy (11.00 wt%).

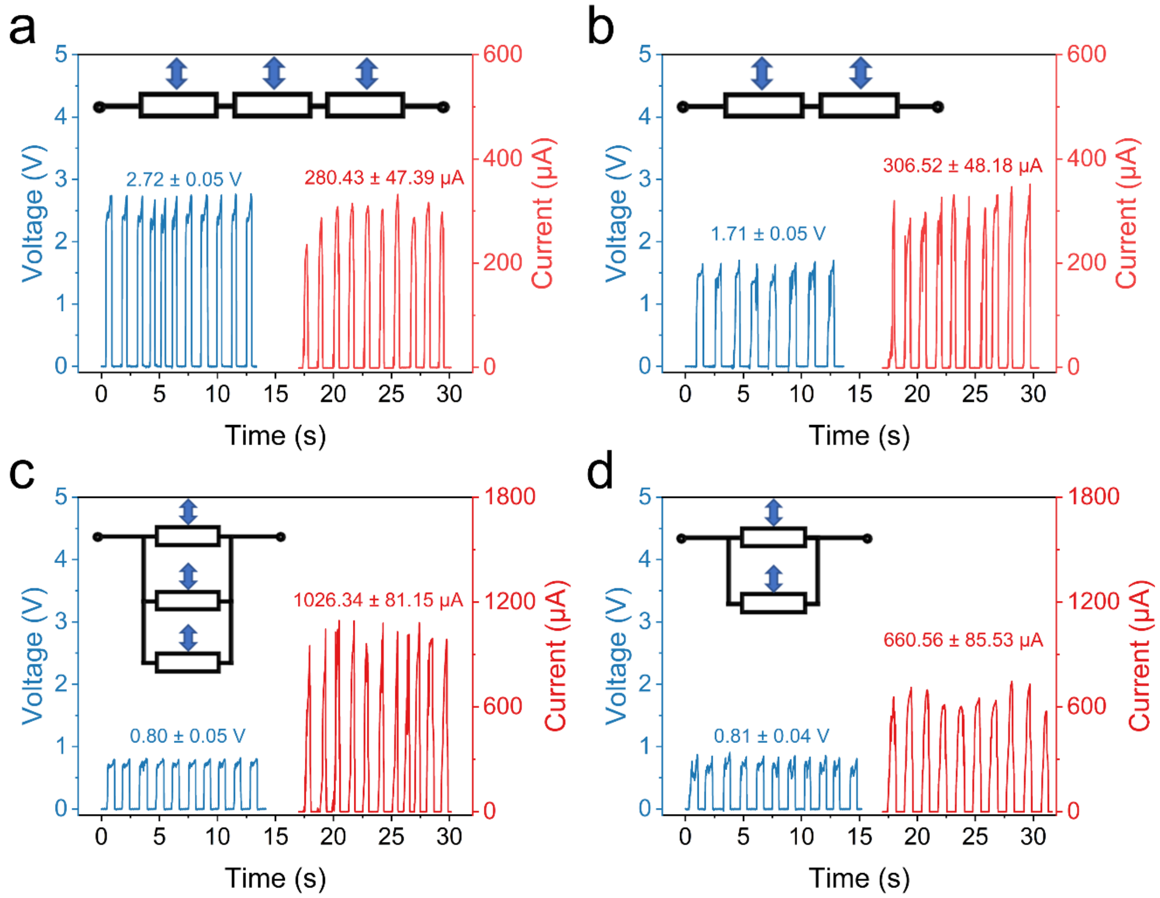

Fig. S18 Electrical outputs of (a) three and (b) two devices series-connected coin devices. Electrical outputs of (a) three and (b) two devices parallel-connected coin devices.

Reference

1 G. Jayakumar, A. A. Irudayaraj and A. D. Raj, *Appl. Phys. A.*, DOI:10.1007/s00339-019-3044-4.

2 C. Dulgerbaki and A. U. Oksuz, *Polym. Adv. Technol.*, 2016, **27**, 73–81.

3 R. D. Sakhare, Y. H. Navale, S. T. Navale and V. B. Patil, *J. Mater. Sci. Mater. Electron.*, 2017, **28**, 11132–11141.